Dielectric, magnetic, and magnetoelectric properties of laminated $PbZr_{0.52}Ti_{0.48}O_3$ / $CoFe_2O_4$ composite ceramics

Jian-ping Zhou, Hong-cai He, Zhan Shi, Gang Liu, and Ce-Wen Nan

Citation: Journal of Applied Physics **100**, 094106 (2006); doi: 10.1063/1.2358191
View online: http://dx.doi.org/10.1063/1.2358191
View Table of Contents: http://aip.scitation.org/toc/jap/100/9
Published by the American Institute of Physics

Dielectric, magnetic, and magnetoelectric properties of laminated $PbZr_{0.52}Ti_{0.48}O_3/CoFe_2O_4$ composite ceramics

Jian-ping Zhou, Hong-cai He, Zhan Shi, Gang Liu,[a] and Ce-Wen Nan[b]
State Key Laboratory of New Ceramics and Fine Processing, Department of Materials Science and Engineering, Tsinghua University, Beijing 100084, People's Republic of China

(Received 16 August 2005; accepted 30 August 2006; published online 9 November 2006)

Multiferroic laminated composites of $PbZr_{0.52}Ti_{0.48}O_3$(PZT)/$CoFe_2O_4$(CFO)/$PbZr_{0.52}Ti_{0.48}O_3$ were prepared by conventional ceramic processing. The interdiffusion of the elements between different layers occurred, altering material properties. The dielectric behavior of such a sandwiched ceramic was dominated by the relative thickness of the different layers because of the high dielectric constant of the PZT layer and the low dielectric constant of the CFO layer. The magnetoelectric behaviors were strongly dependent on the relative thickness of the CFO layer, dc magnetic field, ac magnetic frequency, and the angle θ between the magnetic field and polarization direction. The maximal magnetoelectric-induced voltage coefficient of the composites reaches up to about 27 mV/Oe, close to what was reported previously. The magnetoelectric effect of the laminated composites was also simulated with the finite-element method. The reasons for the difference between experiment and simulation were discussed. © *2006 American Institute of Physics*.
[DOI: 10.1063/1.2358191]

I. INTRODUCTION

In the past decade, multiferroic materials have drawn a continually increasing interest due to their attractive multifunctionality, which provides potential applications in multifunctional devices such as transducers, actuators, and sensors. These materials can produce a dielectric polarization in an external magnetic field, or a magnetization response to an applied electric field, i.e., the magnetoelectric (ME) effect. The ME effect can be expressed by a parameter $\alpha_E \delta E/\delta H$.[1] This effect was observed in single phase Cr_2O_3 as early as 1961.[2] The ME effect in the single phase compounds is weak and commonly appears at low temperature.[3] Alternatively, bulk ME composites,[4–6] such as composites of ferrites and $BaTiO_3$, were proposed due to their higher ME coefficient at room temperature. More recently, giant ME effect was found in piezoelectric/magnetostrictive composites, such as ferrites/Pb(Zr,Ti)O_3(PZT),[7–9] and composites containing Terfenol-D.[10,11]

There are normally some technical obstacles in composing different materials together in bulk, and mostly the ME coefficient is much lower than the theoretical predictions.[1] So far, different kinds of ME composites have been reported. Particulate composites, for example, PZT/$NiFe_2O_4$ (Ref. 7) and Terfenol-D/PZT/polymer,[12] are the easiest to be obtained. Chemical reactions between PZT and ferrites during the sintering process at high temperature change the properties of the piezoelectric and magnetostrictive phases. The large leakage current of the particulate composites makes the electric poling difficult and reduces the ME coefficient because of the low electric resistivity of the magnetostrictive phases.[7] Compared with the particulate composites, the laminated composites exhibit high resistance due to the high resistance of the PZT layer.[8,9] Srinivasan *et al.*[8] reported the bilayers and multilayers of PZT and nickel ferrite by tape casting. Although the microstructures of these bilayers and multilayers are unknown because of no microstructural images in that paper, a large ME coefficient of 460–1500 mV/cm Oe was observed in the nickel ferrite/PZT multilayer stacks.[8] Another very useful coefficient for the ME composites is the magnetoelectric-induced voltage coefficient, i.e., $\alpha_V = \delta V/\delta H = t\alpha_E$, t being the thickness of the materials, related to the output voltage δV, which was used to assess the performance of a ME material for a magnetic sensor.[13,14] The α_V values for the multilayers are in the range of about 0.5–30 mV/Oe after considering their thickness of 10–200 μm.[8] Zhai *et al.* prepared nickel ferrite/PZT composite ceramics with nickel ferrite sandwiched between two PZT layers and also observed a large ME response of about 33 mV/Oe.[9] This is a very simple sandwiched structure, which is easily obtained by a conventional solid state reaction method. However, there easily occurs interdiffusion of elements between PZT and ferrite during the sintering process at high temperature. In comparison with nickel ferrite, cobalt ferrite (CFO) exhibits higher magnetostriction. In this paper, we prepare the sandwiched structure with CFO substitution for nickel ferrite.

The PZT and CFO phases can be bonded together directly to form the laminated composites via a cosintering technique. One key obstacle in preparing the laminated composites by cosintering is the thermal shrinkage mismatch between these two ceramic phases. Through a series of experiments, we obtained the laminated ME ceramic composites with a sandwiched structure, i.e., PZT/CFO/PZT, and mainly studied the element interdiffusion between PZT and CFO,

[a]Present address: State Key Laboratory for Mechanical Behavior of Materials, School of Materials Science and Engineering, Xi'an Jiaotong University, Xi'an 710049, P. R. China.
[b]Author to whom correspondence should be addressed; electronic mail: cwnan@tsinghua.edu.cn

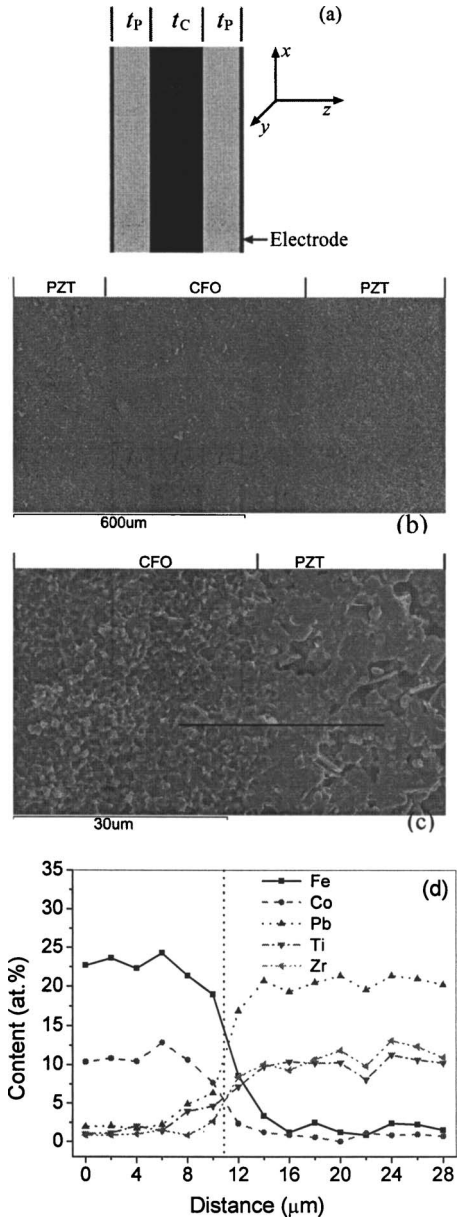

FIG. 1. (a) Schematic illustration of the sandwiched PZT/CFO/PZT composites; [(b) and (c)] SEM micrographs of the fractured surface of the PZT/CFO/PZT sample with $R=2/7$; and (d) element distribution across the boundary, where the upright dot line indicates the average boundary.

and the dielectric, magnetic, and ME properties of the composites. The output voltage induced by the magnetic field is close to what was reported previously. The results were simulated with a finite-element method for better understanding.

II. EXPERIMENT

CFO was selected as the magnetostrictive phase for its largest magnetostriction in the spinel ferrites and PZT as the piezoelectric part. PZT and CFO powders were prepared via a conventional solid state reaction method. These powders were set in a mold with a sandwich structure, with CFO as the inner layer and PZT as the outer layers as shown in Fig. 1(a). The three laminated layers were pressed under 200 MPa to form the green ceramic samples. The diameter and total thickness of the samples were about 10 and 1.8 mm, respectively. The thicknesses of the layers were controlled by the amount of the powders added. The thickness ratio $R=t_C/(2t_P+t_C)$ varies from 1/7 to 5/7, where t_C and t_P denote the thicknesses of CFO and PZT layers, respectively, and the two outer PZT layers were kept at the same thickness. After a series of experiments, a better sintering condition, under which the sandwiched ceramics can be obtained without macrodefects, was selected, i.e., a sintering temperature of 1050 °C under 1 kPa for 4 h. Pure CFO and PZT disks were also sintered at the same condition for comparison.

The sintered samples were polished and coated with silver paste on their surfaces, acting as good electrical contacts for electric measurements. The samples were polarized in silicon oil under an electric field of about 30 kV/cm along the z direction. The piezoelectric constant d_{33} was measured with a standard piezometer. The dielectric properties were measured with an HP4194 impedance analyzer. Magnetostriction measurement was performed under magnetic field of up to 1.5 T with a standard strain gauge technique. Magnetic hysteresis loops were measured with an LDJ9600 type of vibrating sample magnetometer (VSM) for the pure CFO sample and the CFO disk cut from a composite sample. A JSM-6310F type of scanning electron microscope (SEM) equipped with energy dispersive x-ray spectrometer (EDX) was employed to analyze the microstructure and element distribution of the cross section of the samples. The diameter of the spot size for the EDX probe was 1 μm.

The ME effect was measured in terms of the variation of the ME coefficient as a function of dc magnetic field H_{dc}. The sample was put into the dc magnetic field of up to 5.5 kOe superimposed with an ac parallel disturbed magnetic field δH. A signal generator drives the Helmholtz coil to generate the ac magnetic field in the frequency range of 10 Hz–100 kHz. At the output voltage of 20 V, the ac magnetic field generated was variable with frequency because of the coil impendence, for instance, $\delta H=12$ Oe at 1 kHz and $\delta H=3.1$ Oe at 10 kHz. The charges generated from the samples we collected by a charge amplifier (DSC3062, Beijing, China). Then the ME coefficient was obtained with $\alpha_E=\delta E/\delta H=\delta V/t\delta H=\delta Q/\varepsilon_r\varepsilon_0 S\delta H$, where t and S are the thickness and surface area of the samples, E and V are the electric field and voltage induced by the magnetic field, respectively, and ε_r is the relative permittivity. The sample holder can be rotated. When the polarization direction (z direction) was parallel to the magnetic field, i.e., $\theta=0^\circ$, the longitudinal ME sensitivity $\alpha_{E33}(=\delta E_3/\delta H_3)$ was obtained; and when the polarization direction was perpendicular to the magnetic field, i.e., $\theta=90°$, the transverse ME sensitivity $\alpha_{E31}(=dE_3/dH_1)$ was measured.

III. NUMERICAL PROCEDURE

The experimental results were fitted with the finite-element method. The magnetoelectric-elastic effect of composites can be described by[10]

$$\boldsymbol{\sigma} = \mathbf{c}\boldsymbol{\varepsilon} - \mathbf{e}^T\mathbf{E} - \mathbf{c}\boldsymbol{\varepsilon},$$

$$\mathbf{D} = \mathbf{e}\boldsymbol{\varepsilon} + \boldsymbol{\kappa}\mathbf{E} + \boldsymbol{\alpha}\mathbf{H}, \tag{1}$$

$$\mathbf{B} = \mu(\varepsilon, \mathbf{E}, \mathbf{H})\mathbf{H},$$

where $\boldsymbol{\sigma}$ and $\boldsymbol{\varepsilon}$ denote the stress and strain, **D** and **E** are the electric displacement and electric field tensor, and **B** and **H** are the magnetic induction and magnetic field, respectively. **c**, **k**, and μ are the stiffness tensor at constant field, the dielectric constant tensor at constant strain, and the permeability constant tensor at constant strain, respectively. $\boldsymbol{\alpha}$ is the ME parameter, **e** is the piezoelectric coefficient tensor, and $\boldsymbol{\varepsilon}^{\lambda}$ is the magnetostrictive strain of CFO in the magnetic field.

The magnetic flux density in the composites is induced by the external magnetic field, thus the formula can be described with a finite-element form[15]

$$\begin{bmatrix} [K_{uu}] & [K_{u\varphi}] \\ [K_{\varphi u}] & [K_{\varphi\varphi}] \end{bmatrix} \begin{Bmatrix} \{u\} \\ \{\varphi\} \end{Bmatrix} = \begin{Bmatrix} F_u - [K_{uu}]\{\varepsilon^{\lambda}\} \\ Q - [K_{\varphi\theta}]\{\theta\} \end{Bmatrix}, \tag{2}$$

where the submatrices K_{uu}, $K_{u\varphi}$, $K_{\varphi\varphi}$, and $K_{\varphi\theta}$ denote the elastic, piezoelectric, permittivity, and ME coefficient matrices, respectively. F_u and Q indicate the mechanical excitation vector and electric charge vector related to the mechanical loads and electric displacement, respectively.

IV. RESULTS AND DISCUSSION

A. Microstructure and element distribution

Figure 1(b) shows a typical SEM micrograph of the cross section for the PZT/CFO/PZT sample with $R=2/7$. It shows a good sandwiched structure of the composite with clear boundaries and the CFO layer is about 520 μm in thickness, agreeing with the designed thickness. Figure 1(c) further shows the interface region between the PZT and CFO layers. The boundary is still clear. The CFO and PZT layers present different features. EDX analysis was performed along the line shown in Fig. 1(c) across the borderline at the interface. The element distribution was summed up in Fig. 1(d), where the upright dot line indicates the average boundary location. The element atomic ratios at two sides of the boundary are consistent with the formula of $CoFe_2O_4$ and $Pb(Zr_{0.52}Ti_{0.48})O_3$, respectively. The boundary has roughness in microsize, resulting from the coexistence of the two phases, which is about 4 μm in width. Figure 1(d) demonstrates that the interdiffusion of elements between the two layers occurs. The elements Pb, Ti, and Zr diffuse into the CFO layer, while the elements Fe and Co diffuse into the PZT layers when sintered at 1050 °C. The color of the PZT layers become dark in comparison with the yellow of pure PZT bulk for the eye, indicating the diffusion of Co and/or Fe into the PZT layers. The interdiffusion would affect the performance of CFO and PZT. The micrograph in Fig. 1(c) also illustrates that the PZT and CFO layers are not fully densified. A number of pores exist, especially in the PZT layers, because the sintering temperature was not high enough.

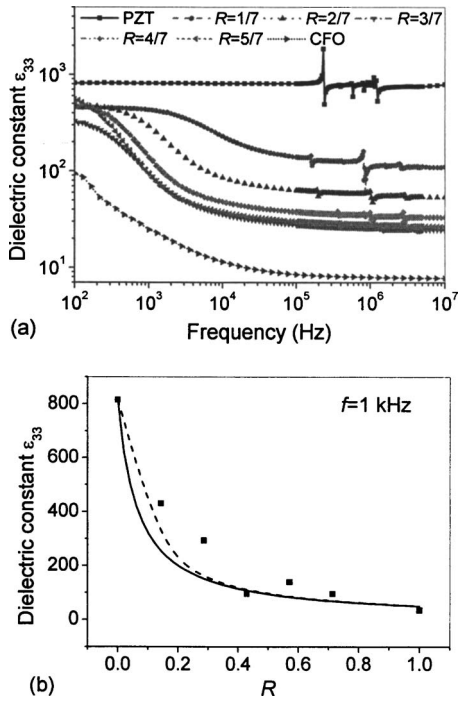

FIG. 2. (a) Frequency dependence of the dielectric constant of the laminated PZT/CFO/PZT ceramics as well as pure PZT and CFO, and (b) dielectric constant as a function of the thickness ratio R for the PZT/CFO/PZT ceramics at 1 kHz, where the dash line is the simulation by using the finite-element method and the solid curve is calculated with Eq. (3).

B. Dielectric and piezoelectric behaviors

PZT is a good dielectric material and its dielectric constant is much larger than that of CFO. As shown in Fig. 2, the dielectric constant of the pure PZT is nearly frequency independent until the electromechanical resonance occurs at about 200 kHz, while that of CFO decreases drastically from 95 to 3 in the frequency range of 100 Hz–100 kHz as reported previously.[16,17] The dielectric constant ε_{33} of the sandwiched ceramics is the combination of the PZT and CFO characteristics. ε_{33} decreases rapidly in a given frequency range, which moves to low frequency with increasing thickness of CFO. The resonance peak at about 200 kHz becomes weaker and weaker with R. The sandwiched PZT/CFO/PZT ceramics can be simply equivalent to three capacitors connected in series. This gives the effective ε_{33} as

$$\varepsilon_{33} = \frac{\varepsilon_C \varepsilon_P}{(1-R)\varepsilon_C + R\varepsilon_P}, \tag{3}$$

where ε_C and ε_P are the dielectric constants of CFO and PZT, respectively. The dielectric constants of the composites were also computed with the finite-element method. As shown in Fig. 2(b), Eq. (3) and the finite-element results are close to each other, but smaller than the experimental data, which might be caused by the possible changes in the dielectric constants of the PZT and CFO layers in the composites due to the interdiffusion of elements (Fig. 1).

Figure 3 shows the variation of the piezoelectric constant d_{33} measured for the laminated PZT/CFO/PZT ceramics with the thickness ratio R. It is well known that PZT has a high piezoelectric constant over 200 pC/N and even higher after

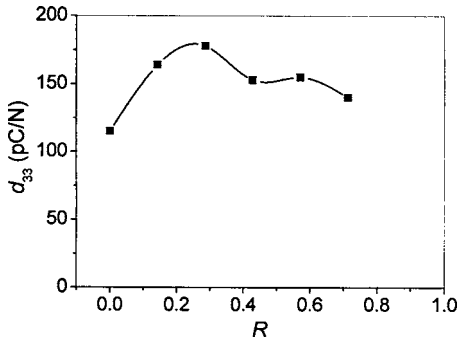

FIG. 3. Piezoelectric constant d_{33} as a function of the thickness ratio R.

doping some elements.[17] The d_{33} value of the pure PZT is about 115 pC/N after sintering at a low temperature of 1050 °C. The low d_{33} value of the PZT is mainly due to pores [Fig. 1(c)]. However, for the composites, d_{33} increases due to the diffusion of Fe and Co elements into the PZT layers. It is worth mentioning that the samples with the thickness ratios $R=1/7$ and $2/7$ show high dielectric constant, low dielectric loss, and high piezoelectric constant.

C. Magnetic behavior

The piezoelectric constant of PZT and the magnetostriction of CFO are two basic parameters that affect the ME effect. Thus the magnetostriction of CFO was measured, too. The strain foil was glued along the x direction in Fig. 1(a). The longitudinal magnetostriction λ_{11} was measured when the strain foil was parallel to the magnetic field, and the transverse magnetostriction λ_{13} was obtained when the strain foil was perpendicular to the magnetic field. The magnetostriction for the pure CFO sintered at 1050 °C was measured as shown in Fig. 4(a). The saturation magnetostriction λ_{11} of

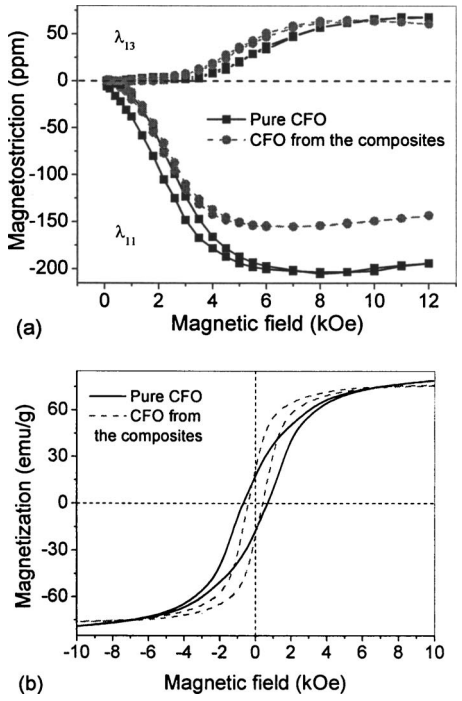

FIG. 4. (a) Magnetostriction and (b) hysteresis loops for the pure CFO sintered at 1050 °C and CFO cut from a composite sample.

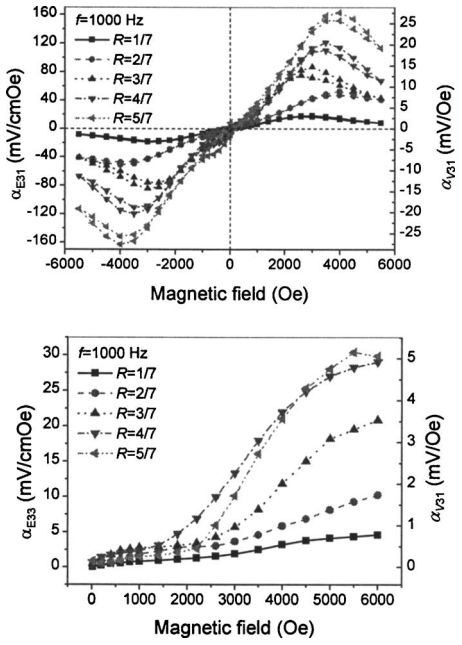

FIG. 5. Transverse magnetoelectric sensitivity α_{E31} and longitudinal magnetoelectric sensitivity α_{E33} of the laminated PZT/CFO/PZT composites as a function of the bias magnetic field measured at 1 kHz. The right axis shows the corresponding magnetoelectric-induced voltage coefficients $\alpha_V = \delta V/\delta H$.

polycrystalline CFO is about −200 ppm, indicating that the saturation magnetostriction of CFO reaches its maximum at this sintering temperature. The loop in the magnetostriction curve shows a typical hard magnetic characteristic. The magnetostriction of the CFO layer cut from one of the composite samples was measured and plotted in Fig. 4(a), too. The diffusion of Pb, Ti, and Zr elements into the CFO layer reduces the saturation magnetostriction λ_{11} to −150 ppm and reduces the magnetic field at the saturation magnetostriction. λ_{13} is much less than λ_{11} as shown in Fig. 4(a) and approaches its saturation at a much higher field.

The magnetic behavior of the samples was also measured by a VSM. Figure 4(b) shows the magnetic hysteresis loops of the pure CFO and the CFO cut from one of the composite samples. The pure CFO shows typical hard magnetic behavior with the coercivity of 650 Oe and the saturation magnetization of 79 emu/g, agreeing with the polycrystalline CFO (i.e., 80 emu/g). After diffusion of a little amount of nonmagnetic elements into CFO, its coercivity decreases at the cost of a little magnetization saturation.

D. Magnetoelectric sensitivity

Figure 5 shows the dc magnetic field dependence of the transverse ME sensitivity α_{E31} and the longitudinal ME sensitivity α_{E33} for the laminated PZT/CFO/PZT ceramics. With increasing magnetic field H_{dc}, α_{E31} increases to its maximum at about 4 kOe and then decreases. In comparison, α_{E33} exhibits a different behavior, and it increases monotonously with the applied magnetic field H_{dc}. For the same sample, α_{E31} is larger than α_{E33}. These characteristics are related to

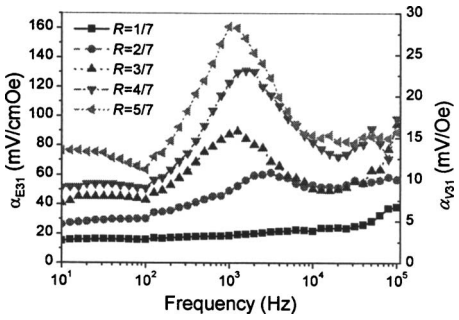

FIG. 6. Variation of the transverse magnetoelectric sensitivity with frequency. The right axis shows the corresponding magnetoelectric-induced voltage coefficients $\alpha_{V31}=\delta V_3/\delta H_1$.

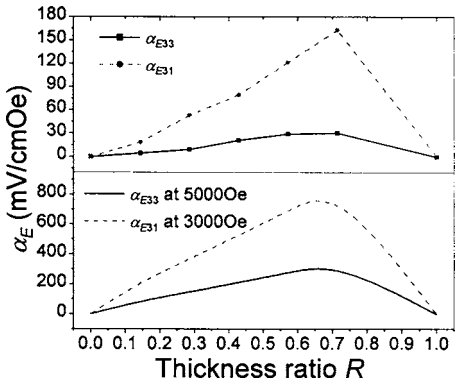

FIG. 7. Magnetoelectric sensitivity as a function of the thickness ratio R at 1 kHz. The upper part shows the experimental results and the lower one is calculated with the finite-element method.

the field dependent magnetostriction shown in Fig. 4(a). λ_{11} reaches its saturation at 5 kOe, and λ_{13} reaches its saturation at 8 kOe out of the ME measurement range.

The transverse ME sensitivity was carefully studied because of its larger values. The ME loops were obtained at around the ME saturation, resulting from the hard magnetic material CFO. The frequency dependence of the transverse ME sensitivity was measured at the α_{E31} maximum and plotted in Fig. 6. With increasing frequency, δQ, ε_r, and δH all decrease. The dielectric constant ε_r of the sandwiched composites exhibit a large decline in the frequency range of 10^2-10^4 Hz [Fig. 2(a)], which results in the wide ME peaks at around 1 kHz from the relation $\alpha_E=\delta Q/\varepsilon_r\varepsilon_0 S\delta H$. The wide ME response peaks of the composites are responsible for high magnetoelectric sensitivity at the low frequency. This frequency dependence of the ME response is quite different from that observed in the PZT/nickel ferrite layered composites,[8,9] which is mainly due to different frequency dependences of the dielectric constants for the cobalt ferrite and nickel ferrite. The maximal ME sensitivity of $\alpha_{E31}=163$ mV/cm Oe is obtained in the composite sample with $R=5/7$. The corresponding magnetoelectric-induced voltage coefficient α_V is shown by the right axis in Figs. 5 and 6. The maximal magnetoelectric-induced voltage ($\alpha_{V31}=27$ mV/Oe) appears at around 1 kHz for the sample $R=5/7$, which is comparable to that in the PZT/nickel ferrite composites[8,9] and that in the sandwiched structure of the PZT-polymer/Terfenol-D-polymer composites measured at nonresonant frequency.[13]

As shown in Figs. 5 and 6, the ME sensitivity is strongly dependent on the thickness ratio R. Figure 7 illustrates the variation of ME sensitivity with R. Both α_{E31} and α_{E33} of the composites nearly linearly increase with the thickness ratio R. This characteristic is similar to that of the PZT-polymer/Terfenol-D-polymer composites.[13]

For better understanding, the results were fitted with the finite-element method. The magnetostrictive behavior of the CFO layer cut from the composite shown in Fig. 5 was used in calculations. The ME coefficient is usually expressed as $\alpha_E=E/H$ in calculations. Then a large α_E corresponds to a larger magnetostrictive coupling coefficient $d=\lambda/H$.[10] The maximum of d was used, i.e., α_{E31} was computed at the magnetic field of 3000 Oe and α_{E33} at 5000 Oe. The boundary conditions of short circuit and ends free in the polarization direction, i.e., $E_3=0$ and $\sigma_{33}=0$ in the z direction shown in Fig. 1(a), were considered to be consistent with the experiment. The data for PZT and CFO used in calculations are listed in Table I (from Refs. 6 and 15). The calculations are shown in the lower part of Fig. 7, which illustrates that the experimental data have the same tendency as the calculations but have lower values. Many factors can influence the ME coefficient, such as the interface coupling. The main reasons for lower measured values than calculated ones are as follows: (1) the cosintering temperature of 1050 °C is lower than the common PZT and CFO sintering temperatures of above ~1200 °C, which results in samples which are not fully dense [Fig. 1(c)] and thus affects their performance; (2) the interdiffusion of the elements between different layers alters the properties of PZT and CFO; and (3) weak interface coupling weakens the ME response observed in the composites.[18] The larger discrepancies shown in Fig. 7 imply that the ME response in the PZT/CFO/PZT sandwiched composites can be further enhanced by optimization of processing of the ceramic composites.

The ME dependence on the angle θ between the polarization direction and the magnetic field direction was investigated. We fixed the magnetic field and changed the polarization direction by rotating the sample along the y direction as shown in Fig. 1(a). The angle variation does not affect piezoelectric properties but changes the magnetostriction, resulting in the ME anisotropy. The anisotropy of the ME coefficient can be expressed as[9]

TABLE I. Properties of PZT and CFO used in the magnetoelectric simulations (Refs. 6 and 15).

Parameter	CFO	PZT
c_{11} (GPa)	267	121
c_{12} (GPa)	154	75.4
c_{33} (GPa)	267	111
c_{44} (GPa)	125	21.1
κ_{11}/κ_0	40	916
κ_{33}/κ_0	40	830
μ_{33}/μ_0	1	1
e_{31} (C/m^2)	0	−5.4
e_{33} (C/m^2)	0	15.8
e_{15} (C/m^2)	0	12.3

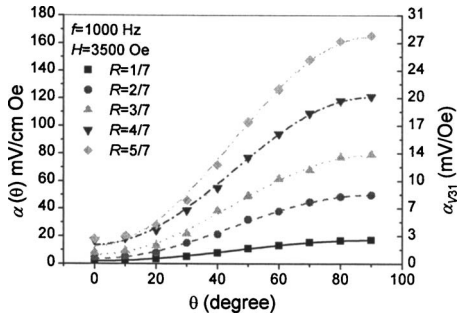

FIG. 8. Dependence of the magnetoelectric coefficient on the angle θ between the polarization and magnetic field. The lines are fitted by using Eq. (4). The right axis shows the corresponding magnetoelectric-induced voltage coefficients $\alpha_V = \delta V / \delta H$.

$$\alpha_E(\theta) \sim A \sin^2(\theta) + B \cos^2(\theta), \tag{4}$$

where A and B are parameters approximately equal to α_{E31} and α_{E33}, respectively. Figure 8 shows the dependence of the ME coefficient on the angle θ measured at 1 kHz and 3500 Oe, as well as their corresponding fitting curves. The right axis shows the corresponding magnetoelectric-induced voltage coefficients α_V. The experimental data at any angle θ lie between α_{E33} and α_{E31}, agreeing with formula (4).

V. CONCLUSIONS

The multiferroic simple sandwiched PZT/CFO/PZT composite ceramics have been prepared via a conventional ceramic sintering process. The maximal magnetoelectric-induced voltage coefficient of the composites reaches up to 27 mV/Oe, close to what was reported previously. The element interdiffusion between different layers during high-temperature processing reduces the saturation magnetostriction and alters the properties of the PZT layer. The ME properties are strongly dependent on the relative thickness of CFO, dc magnetic field, ac magnetic frequency, and the angle θ between magnetic field and polarization direction. The dielectric and ME results of the composites have been simulated with the finite-element method. The results illustrate that further enhancement in the ME response lies in the optimization of processing the simple structured ceramic composites.

ACKNOWLEDGMENTS

This work was supported by the State Key Project of Fundamental Research of China (Grant No. 2002CB613303) and the National Natural Science Foundation of China (Grant Nos. 50232030, 50318002, and 50328203).

[1] See, for example, M. Fiebig, J. Phys. D **38**, R123 (2005).
[2] V. J. Folen, G. T. Rado, and E. W. Stalder, Phys. Rev. Lett. **6**, 607 (1961); G. T. Rado and V. J. Folen, *ibid.* **7**, 310 (1961).
[3] See, for example, T. Lottermoser, T. Lonkai, U. Amann, D. Hohlwein, J. Ihringer, and M. Fiebig, Nature (London) **430**, 541 (2004).
[4] J. van Suchtelen, Philips Res. Rep. **27**, 28 (1972).
[5] G. Harshe, J. P. Dougherty, and R. E. Newnham, Int. J. Appl. Electromagn. Mater. **4**, 161 (1993).
[6] C. W. Nan, Phys. Rev. B **50**, 6082 (1994).
[7] J. Ryu, A. V. Carazo, K. Uchino, and H.-E. Kim, J. Electroceram. **7**, 17 (2001).
[8] G. Srinivasan, E. T. Rasmussen, J. Gallegos, R. Srinivasan, Y. I. Bolhan, and B. M. Laletin, Phys. Rev. B **64**, 214408 (2001); G. Srinivasan, E. T. Rasmussen, and R. Hayes, *ibid.* **67**, 014418 (2003).
[9] J. Y. Zhai, N. Cai, Z. Shi, Y. H. Lin, and C. W. Nan, J. Appl. Phys. **95**, 5685 (2004).
[10] C. W. Nan, M. Li, X. M. Feng, and S. Yu, Appl. Phys. Lett. **78**, 2527 (2001); C. W. Nan, M. Li, and J. H. Huang, Phys. Rev. B **63**, 144415 (2001).
[11] S. Dong, J. Cheng, J. F. Li, and D. Viehland, Appl. Phys. Lett. **83**, 4812 (2003); S. Dong, J. F. Li, and D. Viehland, *ibid.* **85**, 5305 (2004).
[12] C. W. Nan, L. Liu, N. Cai, J. Zhai, Y. Ye, Y. Lin, L. J. Dong, and C. X. Xiong, Appl. Phys. Lett. **81**, 3831 (2002); C. W. Nan, N. Cai, L. Liu, J. Zhai, Y. Ye, and Y. Lin, J. Appl. Phys. **94**, 5930 (2003).
[13] C. W. Nan, N. Cai, Z. Shi, J. Zhai, G. Liu, and Y. Lin, Phys. Rev. B **71**, 014102 (2005).
[14] S. Dong, J. Zhai, F. Bei, J. F. Li, and D. Viehland, Appl. Phys. Lett. **87**, 062502 (2005).
[15] G. Liu, C. W. Nan, N. Cai, and Y. H. Lin, J. Appl. Phys. **95**, 2660 (2004).
[16] M. S. Selim, G. Turky, M. A. Shouman, and G. A. El-Shobaky, Solid State Ionics **120**, 173 (1999).
[17] A. Garg and D. C. Agrawal, J. Mater. Sci.: Mater. Electron. **10**, 649 (1999).
[18] M. I. Bichurin, V. M. Petrov, and G. Srinivasan, J. Appl. Phys. **92**, 7681 (2002).